JTTEE5 18:194–200
DOI: 10.1007/s11666-009-9310-9
1059-9630/$19.00 © ASM International

Microindentation and Inverse Analysis to Characterize Elastic-Plastic Properties for Thermal Sprayed Ti_2AlC and NiCoCrAlY

J. Jiang, A. Fasth, P. Nylén, and W.B. Choi

(Submitted October 15, 2008; in revised form February 16, 2009)

Elastic-plastic material properties for HVOF sprayed Ti_2AlC (sprayed with Maxthal 211 powder) and plasma sprayed NiCoCrAlY coatings were investigated using modeling and experimental Berkovich microindentation. Optical microstructure evaluations were also performed. The theories of Hertz, Oliver and Pharr were combined with finite element analysis for extracting the material properties. Empirically based material models for both thermal sprayed Ti_2AlC and NiCoCrAlY coatings are proposed.

Keywords elastic-plastic properties, indentation, inverse analysis, MAX phase, NiCoCrAlY

1. Introduction

Ti_2AlC is a member of the $M_{n+1}AX_n$-phase family (Ref 1), which consists of ternary compounds where M corresponds to an early transition metal (M), such as Ti or V, combined with a p-element from group III-X to IIII-X (A groups) and C and/or N(X). The phases have a layered structure in which the A element forms planes separated by MX slabs. This nanolaminated atomic arrangement gives rise to a unique set of properties (Ref 1). Bulk Ti_2AlC shows thermal expansion coefficient equal to $8.8 \pm 0.2 \times 10^6$/K, and thermal conductivity at 1300 K is 36 W/m K (Ref 1). In combination with a good match in thermal expansion between substrate and coating, these properties make the extension of the lifetime of thermal barrier coatings using MAX-phase materials, as bondcoats, very challenging.

Research on MAX-phase materials is rather limited. Barsoum et al. (Ref 1, 2) have thoroughly investigated the properties of hot isostatic pressed (HIP) MAX phase, classifying it as room-temperature ductile carbides because of its rather unique deformation mechanism. Hultman et al. have used magnetron sputtering to produce MAX-phase thin films (Ref 3). The work presented here is part of an ongoing project aimed at investigating, both experimentally and by modeling, the properties of MAX-phase materials starting with Ti_2AlC and later also including Ti_3SiC_2. Particular focus is placed on mechanical modeling and the development of a HVOF spray method to produce comparatively thick (approximately 130 μm) bond coatings.

The performance and reliability of thermal barrier systems are greatly affected by the behavior of the bond coat. The surface texture of the bond coat improves the adhesion of the ceramic topcoat, and thermal mismatch leads to improved oxidation resistance and reduced stresses between topcoat and substrate. Elastic-plastic properties are relevant for the survivability of these coatings. Hence, knowledge of the elastic-plastic properties of coatings is of great interest in scientific studies dealing with residual stresses, thermal mismatch, or fracture mechanics, as well as in engineering for dimensioning components. In this article, modeling of mechanical properties for such coatings is presented. A comparison of material behavior between a MAX-phase, namely Ti_2AlC, coating and one of the most commonly used materials in aerospace bond coatings, namely NiCoCrAlY, is provided. Empirically based material models for thermal spray Ti_2AlC and NiCoCrAlY are also suggested. The empirical models are based on experimental results combined with finite element modeling. Additionally, metallographic investigations of both materials were also pursued. Hastelloy-X was chosen as substrate material in the investigation. A similar modeling approach for NiCrAlY and Ni-Al bondcoats, as well as WC-Co cermet coatings can be found in Ref 4 and 5.

2. Experimental Procedure

2.1 Sample Fabrication

The Ti_2AlC powder used was MAXTHAL 211, developed by Kanthal AB, Halstahammar, Sweden. The morphology and the grain structure of the powder fabricated for this investigation is shown in Fig. 1.

MAX-phase crystals have hexagonal structures and contain TiC layers interleaved with single Al layers. The

J. Jiang, A. Fasth, and **P. Nylén**, University West, Trollhättan, Sweden; and **W.B. Choi**, Center for Thermal Spray Research, Stony Brook, NY. Contact e-mail: janna.jiang@hv.se.

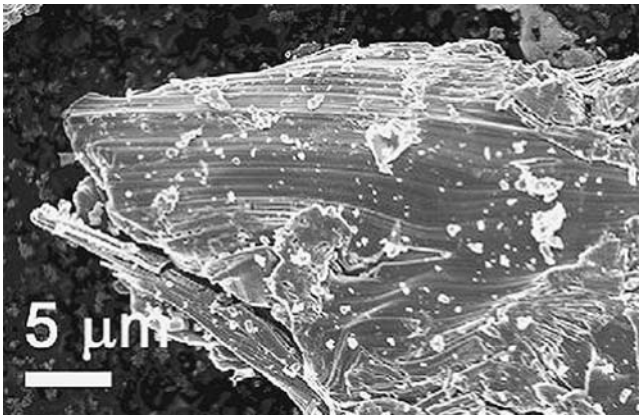

Fig. 1 SEM image of flakelike grain in the Ti_2AlC powder (Ref 6)

Table 1 HVOF process parameter for MAX-phase coatings

Gun	Diamond jet 2600
Primary gas, nL/min	Hydrogen, 505
Secondary gas, nL/min	Oxygen, 149
Shrouding gas, nL/min	Air, 360
Carrier gas, L/min	Argon, 23.2
Spray distance, mm	230

stacking sequence depends on the stoichiometry where Ti_2AlC, has one Al layer for every second TiC layer. The atomic binding character in these MAX phases has been shown to be metallic, ionic, and covalent (Ref 7). The covalent-ionic Ti-C bonds are comparable to the bonds in the binary TiC and are stronger than the metallic Ti-Al bonds present in the ternary structure (Ref 8). The relatively weak bonds between the TiC and Al layers (basal planes) contribute to an anisotropic character of the material leading to kink-band formation and delaminations along the basal planes upon deformation (Ref 9). The basal planes are clearly shown in Fig. 1. The average diameter for the powder in this investigation was 46 µm. The NiCoCrAlY feedstock material was the commercially available powder AMDRY 356-2 from Sulzer Metco (Wohlen, Switzerland), which is commonly used in the aerospace industry.

Both the NiCoCrAlY and the MAX-phase coating were sprayed onto Hastelloy X substrates with dimensions $100 \times 20 \times 1.6$ mm^3. The substrate surface was cleaned with acetone and then grit blasted with grit 60 alumina grit using a pressure of 4 bar. The NiCoCrAlY coatings were then atmospheric plasma sprayed (APS) (Plasma-Technik A3000S, Sulzer Metco AG, Wohlen, Switzerland). The Maxthal powder was sprayed using the Sulzer Metco HVOF hybrid DJ-2600 gun. Oxygen/hydrogen gases were chosen as the oxyfuel mixture. The HVOF and APS parameter settings are listed in Table 1 and 2, respectively.

The APS process was chosen for the NiCoCrAlY coatings since it was decided to use an industrial standard as reference. The HVOF process was chosen for the MAX-phase coating since, compared to APS spraying, this process offers a lower particle temperature in combination with a higher particle velocity (Ref 6). This lower particle temperature and shorter residence time reduces the degree of melting and oxidation of the powder. Measurements of particle in-flight properties were performed using the DPV2000 system (Ref 10), using autocentering. Average values of measured properties are provided in Table 3.

Table 2 APS process parameter for NiCoCrAlY coatings

Plasma gun	F4
Arc effect, kW	42
Plasma rate flow rate, nL/min	56.8
Powder feed rate, g/m	60
Spray distance, mm	135
Carrier gas flow rate, nL/min	Argon, 2.8

Table 3 DPV2000 measurements for HVOF MAX-phase experiments

Speed, m/s	Standard deviation, ±	Temperature, °C	Standard deviation, ±	Diameter, µm	Standard deviation, ±
719	13	2111	18	44	1

2.2 Metallographic Investigation

Metallographic investigation of sprayed coatings revealed unmelted powder grains of Ti_2AlC embedded in the coating (Fig. 2). There are three ternary phases within the Ti-Al-C system. The interface between the coating and substrate is compact with no voids or delaminations detected. Of the three phases, two are MAX phases, namely Ti_2AlC and Ti_3AlC_2, while the third is a perovskite, Ti_3AlC. X-ray diffraction (XRD) from earlier studies (Ref 6) was used to detect minority phases of Ti_3AlC_2, TiC, and Al_xTi_y alloys. X-ray pole figure measurements revealed a preferred crystal orientation in the coatings with the Ti_2AlC (000l) planes aligned to the substrate surface.

2.3 Mechanical Characterization

Microindentation was performed with an instrumented indenter Micro test (Micro Materials Limited, Wrexham, UK). The experiment was displacement controlled with an indentation velocity of 3.8 µm/s. When the maximum available depth was reached, the indenter was held for 15 s and then moved back with the same speed. A total of 15 indentations were made for each sample. A Berkovich indenter was used on both coatings with a maximum load of 5 N (Fig. 3).

No evaluations of anisotropic effects were included in the present study. The substrate was assumed to be elastic since it was never subjected to any substantial stresses during the indentation of interest. The Berkovich indenter is composed of a diamond.

The load-displacement curve was recorded continuously and elastic modulus determined from the unloading curve according to the Oliver and Pharr method (Ref 11) (Fig. 4).

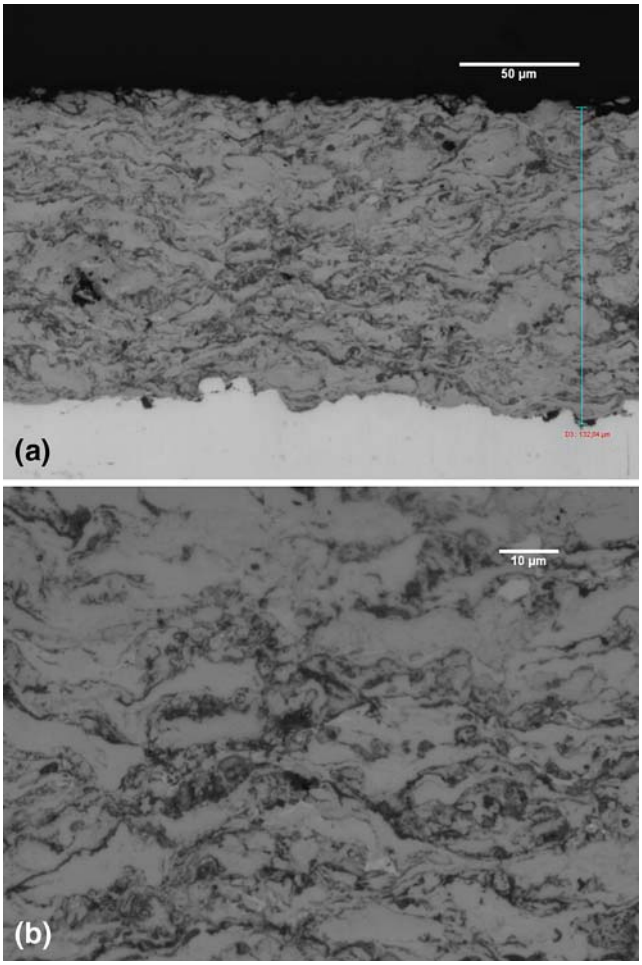

Fig. 2 Optical microscope cross section of HVOF sprayed MAX-phase coating. Original magnification: (a) 200× and (b) 500×

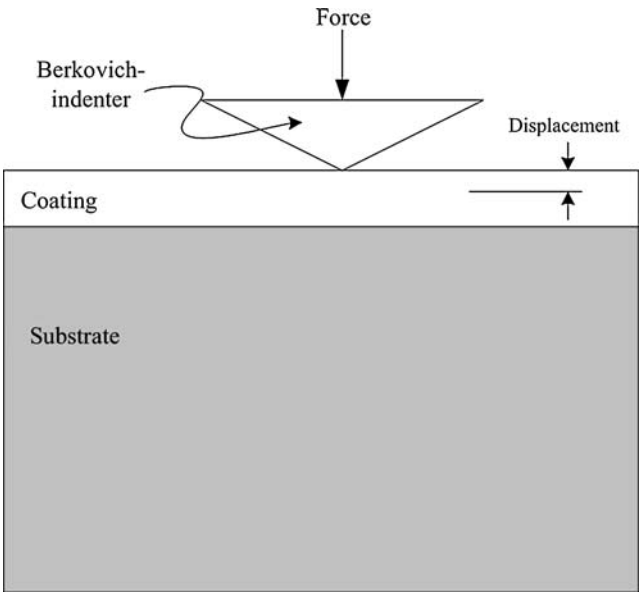

Fig. 3 Berkovich microindentation of a thermal sprayed coating on 2-mm thick Hastelloy-X substrate

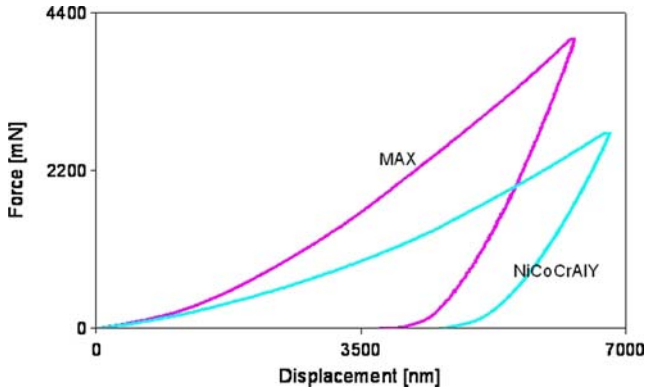

Fig. 4 Determined load-displacement curves from indentation tests on MAX-phase and NiCoCrAlY coatings

3. Analysis Procedure

The Oliver-Pharr method (Ref 11) was used to determine the elastic modulus for the elastic part of the constitutive relation. The plastic properties of the coatings were determined by solving the inverse problem using a two-dimensional finite element analysis (FEA) model. For this purpose, the determined elastic modulus was given as input in the FEA model with a stress-strain curve first assumed as an initial constitutive relation for the coating. A load-displacement curve was then predicted using the model. The predicted load-displacement curve was then compared with the experimental load-displacement curve, and the constitutive curve was iteratively modified until a best fit was reached (Fig. 5).

4. FEA Model

4.1 Numerical Model

The overall objective with the FEA model is to predict the elastic-plastic material behavior, namely, stress-strain relationship based on load-displacement relationships determined through indentation, that is, through inverse analysis. The sample was modeled using a two-dimensional axisymmetric mesh. The three-sided pyramid indenter was substituted by an axisymmetric cone with a semi-angle of 70.3°. This angle was chosen since it gives the same area-to-depth ratio as the pyramid-shaped Berkovich indenter, which is not axisymmetric. The projected area of contact was chosen, instead of the actual area, since it has been shown to give more accurate results. The FEA software Marc from MSc Software (Gothenburg, Sweden) was used. It should also be noted that FEA simulations of indentation experiments require a nonlinear formulation. The problem is generally nonlinear in three ways: (a) large strains under the indenter necessitate frequent updates to all nodes in the mesh, (b) material properties are nonlinear due to plasticity, and (c) contact between the indenter and the sample produces nonlinear boundary conditions.

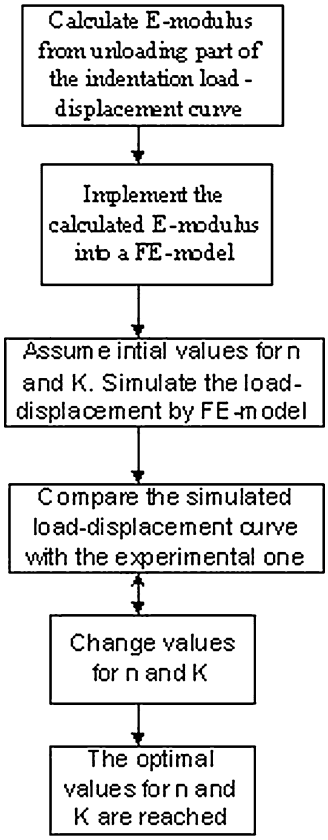

Fig. 5 Flow chart of the analysis procedure to determine elastic-plastic parameters

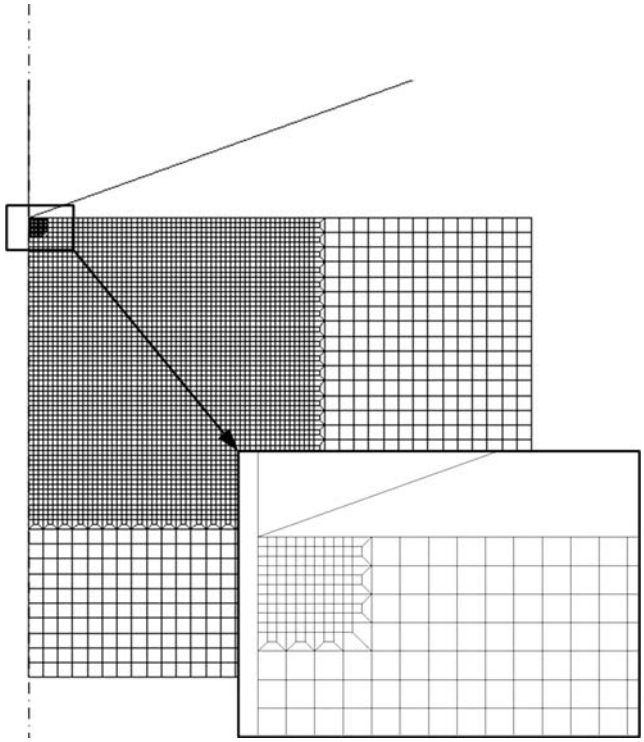

Fig. 6 The axisymmetric finite element mesh. The near-contact region with higher mesh density enlarged

An updated Lagrangian formulation was used to handle the potentially large strains. The solution was determined in discrete time steps. The indenter was treated as a rigid body, and the sample was modeled using eight-node's second-order axisymmetric elements. Modeled coating thickness was 134 μm and thickness of substrate 2 mm. The boundary conditions were specified in the following way. First, along the horizontal bottom line of the sample, the displacements (u_x) were set to zero. Then, along the axis of symmetry, that is, the left side of the sample, nodes were constrained to move along the axis of symmetry only ($u_y = 0$).

The indenter (Fig. 3) moves downward by 3 μm per second. Rigid body movement was constrained in all other directions. A higher mesh density was used at the indenter-coating contact region to more accurately predict stress and strain, and to obtain a smoother force-displacement curve (Fig. 6).

4.2 Material Model

The Ramberg-Osgood model:

$$\varepsilon = \varepsilon_e + \varepsilon_p = \frac{\sigma}{E} + \left(\frac{\sigma}{K}\right)^{1/n}$$

was chosen to describe the Ti_2AlC and NiCoCrAlY coatings. In this model, the elastic and plastic strains, ε_e and ε_p are considered separately and summed. An exponential relationship was assumed between the plastic strain and stress. In the Ramberg-Osgood model, three parameters need to be determined: the elastic modulus that was determined in the experiments; the parameter n, which is the strain-hardening exponent that has been shown to vary in the range from 0.01 to 0.5 for metallic materials; and, finally, the parameter K, which is structure dependent and influenced by processing conditions. K and n were determined by the inverse iterative method described previously. The MAX-phase and NiCoCrAlY coatings were modeled as isotropic, elastic-plastic solid materials that obey von Mises yield criterion with isotropic hardening. ν was set to 0.2 in the analysis, which was derived from the literature for bulk MAX-phase material (Ref 1) and 0.3 for NiCoCrAlY.

5. Results

The load P versus displacement h curves were fitted according to the Oliver and Pharr method (Ref 11). The elastic modulus was determined from the elastic recovery part of the unloading curve, which relates the modulus, E, to the initial loading stiffness, S:

$$S = \frac{dP}{dh} = \frac{2}{\sqrt{\pi}} E^* \sqrt{A}$$

Table 4 Elastic modulus calculated for NiCoCrAlY from Berkovich indentation

Indent	1	2	3	4	5
E, GPa	42	68	49	71	68
Indent	**6**	**7**	**8**	**9**	**10**
E, GPa	72	67	66	72	64
Indent	**11**	**12**	**13**	**14**	**15**
E, GPa	63	65	50	65	67

Table 5 Elastic modulus calculated for MAX-phase coating from Berkovich indentation

Indent	1	2	3	4	5
E, GPa	106	107	99	84	92
Indent	**6**	**7**	**8**	**9**	**10**
E, GPa	111	91	119	98	97
Indent	**11**	**12**	**13**	**14**	**15**
E, GPa	97	97	95	89	98

where E^* is the reduced elastic modulus and A is the projected area under the indenter tip. The reduced modulus is related to the sample modulus by:

$$\frac{1}{E^*} = \frac{(1-\nu^2)}{E} + \frac{(1-\nu'^2)}{E'}$$

where E and ν are the elastic modulus and Poisson's ratio of the specimen and E' and ν' are the corresponding values for the diamond indenter.

The values of the elastic module obtained for both coatings are summarized in Table 4 and 5. The elastic modulus for thermal sprayed MAX-phase coatings is around 100 GPa, and for NiCoCrAlY is around 60 GPa.

By using the least squares curve fit, parameters K and n were determined. It should be noted that for metallic materials, n ranges from 0.01 to 0.5, for the MAX-phase material the nonlinear part begins earlier because of the ceramic behavior, which explains why n is bigger than 0.5 and less than 1 for this material.

As shown in Fig. 7, even with the best-fit parameters there is a deviation between the simulated load-displacement curve and the corresponding experimental one. This is probably because the rather simple assumed material model, namely, this material, is based on the assumption that the MAX phase behaves isotropically. As described in the introduction, the MAX phase material is not an isotropic material and shows texture effects in the HVOF coating (Ref 4). Therefore, even for the multicrystalline coating an isotropic material model cannot be expected to describe the behavior completely. To better catch the real material behavior, the dynamic behavior during deformation can be included by adding, for example, relaxation terms and pileup dependent terms.

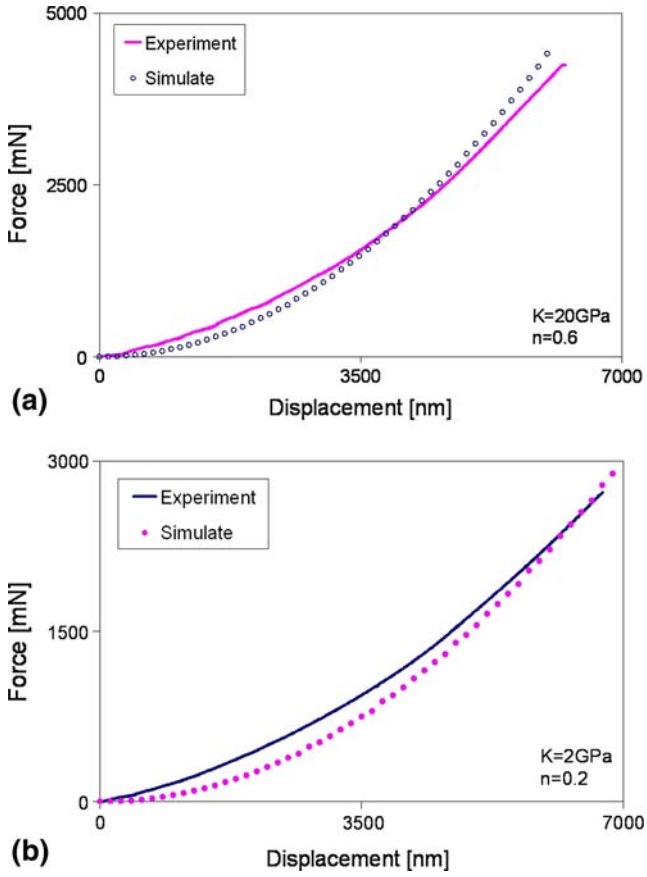

Fig. 7 Comparison between the simulated and the measured data for (a) MAX-phase coating and (b) NiCoCrAlY

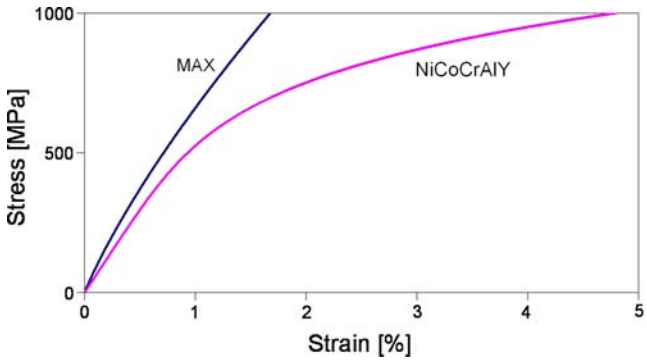

Fig. 8 The proposed constitutive relation for HVOF sprayed MAX phase and plasma sprayed NiCoCrAlY

The proposed material models are shown in Fig. 8. The stress-strain curve for the HVOF sprayed MAX-phase material is nearly linear. It should be remembered that the x-ray diffraction (XRD) from earlier studies (Ref 6) detected minority phases of Ti_3AlC_2, TiC, and Al_xTi_y alloys in the sprayed coatings, which might explain the deviation from linearity by the formation of microcracks during

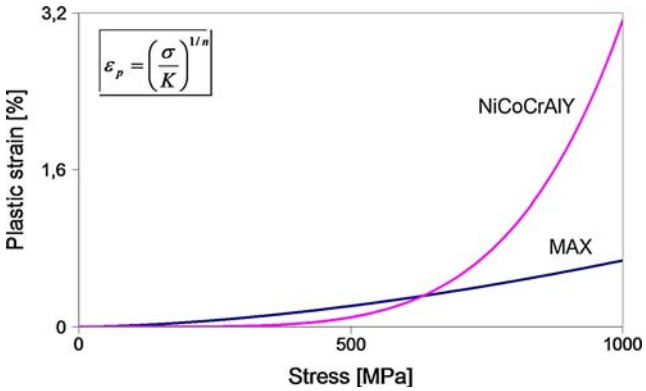

Fig. 9 Stress-plastic strain curves for MAX phase and NiCoCrAlY

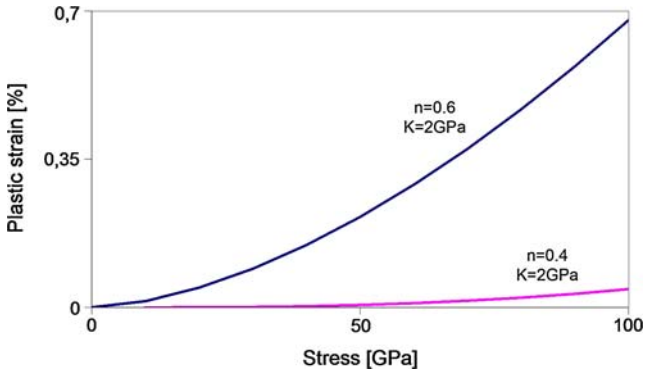

Fig. 10 Stress-plastic strain curves for two different materials with same K values but different n

indentation and/or the nonlinear elastic deformation (Ref 1) of the phases (Ti_2AlC and Ti_3AlC_2). NiCoCrAlY behaves as a metal with a strain-hardening coefficient of 0.4. It also shows a distinct yield stress level. The plastic strain grows much slower for NiCoCrAlY as can be seen in Fig. 9.

6. Discussion

A study was finally performed to evaluate the sensitivity against assumed and determined parameters. In Fig. 10, two stress-strain curves with the same K value and the same ν, but with a different n, is given, n prescribes the rate at which the plastic strain grows. The material with $n = 0.4$ has almost no plastic strain during low stress, while the material with $n = 0.6$ deforms plastically almost immediately right at the beginning; that is, the material behavior is very sensitive to this parameter.

Another important parameter is the Poisson's ratio ν, which is also a critical parameter for plastic properties. For thermal sprayed coatings, ν is an unknown parameter due to coating heterogeneity. For NiCoCrAlY two values were found in literature, namely 0.25 given by Nakamura et al. (Ref 12) and 0.33 by Zhu et al. (Ref 13). In this study, 0.3 was chosen.

Errors as a function of n and K are shown in Fig. 11. The chosen optimized n, K minimize errors, and they give the best overall fitness of the force and displacement curve. Isocontours of equivalent plastic strains for the two materials are presented in Fig. 12. The elastic modulus is higher for the MAX-phase coating; thus even with bigger value on n, MAX phase still shows a smaller equivalent plastic strain.

It should be noted that characterization of mechanical properties for heterogeneous coatings is difficult, which means that the results have to be interpreted carefully. MAX-phase coating is previously stated heterogeneous both in the respect that the slip planes orientation and the respect to the minor phases within the coating. Another factor that needs to be taken into account is that the proposed models are based on a series of assumptions.

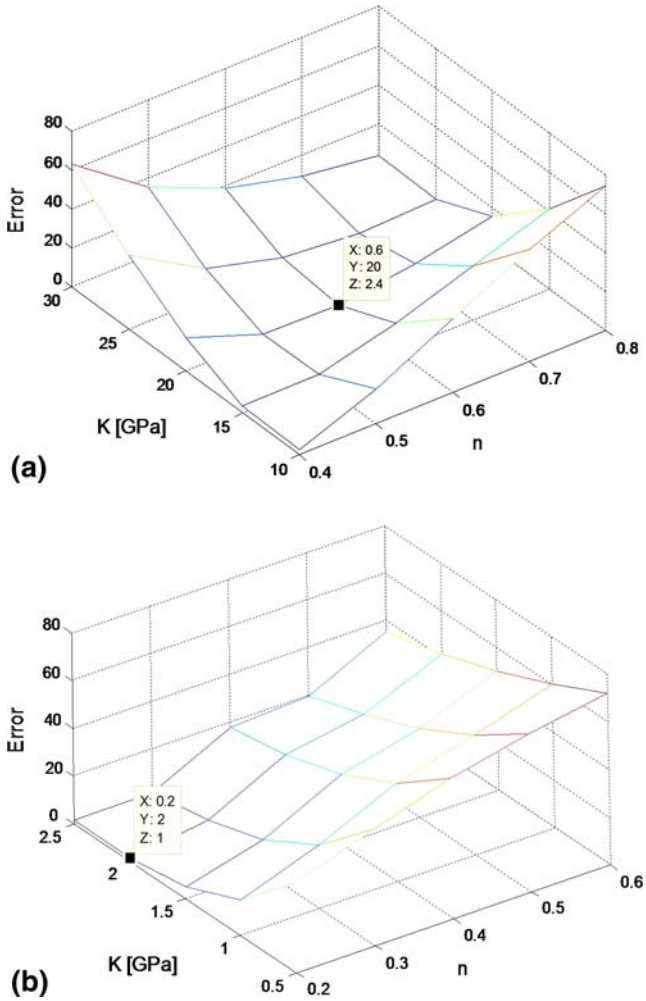

Fig. 11 Errors derived using least square method are shown as a function of n and K for (a) MAX-phase and (b) NiCoCrAlY coating. The error surface is constructed with interpolation

When using the FE model, we assume that the inhomogeneous coatings behave as a continuum, and we have not taken account of either pileups or the fact that the Ramberg-Osgood model might be too simple to catch the dynamic deformation during indentation.

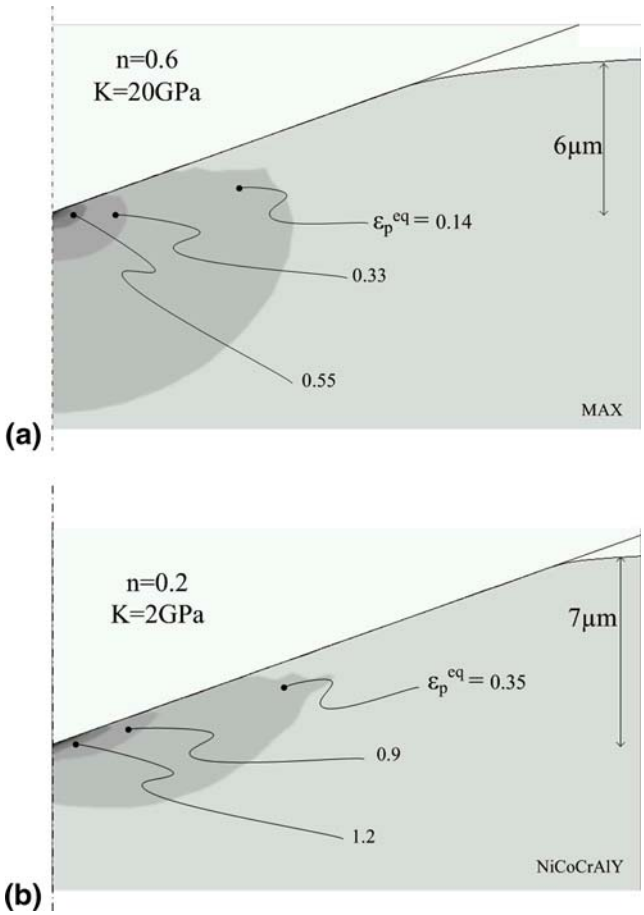

Fig. 12 Shades of equivalent plastic strain from finite element simulation on (a) MAX-phase and (b) NiCoCrAlY coating. Darker regions correspond to higher plastic strain

No papers have been found to compare the results with. Most of the papers currently written have the aim of determining elastic properties only. However, for our semiceramic MAX-phase coating it is, we believe, more interesting to see the overall behavior between a bigger strain interval, since the bulk phase shows a highly unique stress-strain behavior during compression testing.

7. Conclusion and Future Work

The aim this work was to validate and compare the mechanical material properties for MAX-phase and NiCoCrAlY coatings. The overall conclusion from the study was that the MAX-phase coating behaves more like a ceramic with a higher elastic modulus and with no pronounced yield stress level in relation to the NiCoCrAlY coating. The reason for this will thus be investigated further, but one possible explanation could be that most of the aluminum transforms to Al_xTi_y during the spray process, which the metallographic investigation indicated. With the aim of preserving the content of MAX phase, the spray parameters have to be optimized. SEM studies on the indentation marks are necessary to take a closer look at the deformation mechanism. To confirm the proposed material models, additional tests have to be done such as, for example, by four-point bending. Further indentation tests on different depths with another indenter and from a different direction would also be of interest.

Oxidation of HVOF sprayed MAX-phase coating in the temperature range 700-1200 °C have been studied in an ongoing parallel project (Ref 14). Results from this study show that because of the presence of TiC and Ti_xAl_y and the occurrence of pores in the coating, a protective layer of aluminum oxide does not form. Instead, internal oxidation throughout the coating was observed. Thus optimization of the spray parameters is necessary. Evaluation of the thermal properties is also on-going in parallel.

Despite these facts, the results indicate that MAX-phase coatings have interesting properties that make them worthy of further evaluation as bondcoat materials.

References

1. M.W. Barsoum, The Mn + 1AXn Phases: A New Class of Solids; Thermodynamically Stable Nanolaminates, *Prog. Solid State Chem.*, 2000, **28**, p 201-281
2. M.W. Barsoum and T. El-Raghy, Synthesis and Characterization of a Remarkable Ceramic: Ti_3SiC_2, *J. Am. Ceram. Soc.*, 1996, **79**(7), p 1953-1956
3. H. Högberg, J. Hultman, T. Emmerlich, T. Joelsson, P. Eklund, J.M. Molina-Aldareguia, J.-P. Palmquist, O. Wilhelmsson, and U. Jansson, Growth and Characterization of MAX-Phase Thin Films, *Surf. Coat. Technol.*, 2005, **193**(1-3), p 6-10
4. W.B. Choi, L. Prchlik, S. Sampath, and A. Gouldstone, Indentation of Metallic and Cermet Thermal Spray Coatings, *J. Therm. Spray Technol.*, 2008, **18**(1), p 58-64
5. W.B. Choi, Y. Wu, S. Sampath, and A. Gouldstone, Modified Indentation Techniques to Probe Inelasticity in Ni-5%Al Coatings from Different Processes, *J. Therm. Spray Technol.*, 2008, **18**(1), p 65-74
6. J. Frodelius, M. Sonestedt, S. Björklund, J.-P. Palmquist, K. Stiller, H. Högberg, and L. Hultman, Ti_2AlC Coatings Deposited by High Velocity Oxy-Fuel Spraying, *Surf. Coat. Technol.*, 2008, **202**(24), p 5976-5981
7. Y. Zhou and Z. Sun, Electronic Structure and Bonding Properties of Layered Machinable Ti_2AlC and Ti_2AlN Ceramics, *Phys. Rev. B*, 2000, **61**, p 12570-12573
8. Z. Sun, D. Music, and R. Ahuja, Bonding and Classification of Nanolayered Ternary Carbides, *Phys. Rev. B*, 2004, **70**, p 092102
9. Y.C. Zhou and X.H. Wang, Deformation of Polycrystalline Ti_2AlC under Compression, *Mater. Res. Innovat.*, 2001, **5**(2), p 87-93
10. C. Moreau, P. Gougeon, M. Lamontagne, V. Lacasse, G. Vaudreuil, and P. Cielo, On-Line Control of the Plasma Spraying Process by Monitoring the Temperature, Velocity and Trajectory of In-Flight Particles, *Thermal Spray Industrial Applications: Proc. Seventh National Thermal Spray Conference* (Boston, MA), 1994, p 431-437
11. A.C. Fischer-Cripps, A Review of Analysis Methods for Submicron Indentation Testing, *Vacuum*, 2000, **58**(4), p 569-585
12. T. Nakamura, T. Wang, and S. Sampath, Determination of Properties of Graded Materials by Inverse Analysis and Instrumented Indentation, *Acta Mater.*, 2000, **48**(17), p 4293-4306
13. H.X. Zhu, N.A. Fleck, A.C.F. Cocks, and A.G. Evans, Numerical Simulations of Crack Formation from Pegs in Thermal Barrier Systems with NiCoCrAlY Bond Coats, *Mater. Sci. Eng. A*, 2005, **404**(1-2), p 26-32
14. M. Sonestedt, "Microstructure and Oxidation Behavior of High Velocity Oxy-Fuel Spray Deposited Ti_2AlC Coatings," Licentiate thesis, 2008